Processes for design, construction and utilisation of arrays of light-emitting diodes and light-emitting diode-coupled optical fibres for multi-site brain light delivery

Jacob Gold Bernstein[1,2], Brian Douglas Allen[1,2], Alexander A. Guerra[1], Edward Stuart Boyden[1,2,3]

[1]*The MIT Media Lab, Massachusetts Institute of Technology, Cambridge, MA 02139, USA*
[2]*Department of Brain and Cognitive Sciences and MIT McGovern Institute for Brain Research, Massachusetts Institute of Technology, Cambridge, MA 02139, USA*
[3]*Department of Biological Engineering, Massachusetts Institute of Technology, Cambridge, MA 02139, USA*
E-mail: esb@media.mit.edu

Published in *The Journal of Engineering*; Received on 5th November 2014; Accepted on 31st March 2015

Abstract: Optogenetics enables light to be used to control the activity of genetically targeted cells in the living brain. Optical fibres can be used to deliver light to deep targets, and light-emitting diodes (LEDs) can be spatially arranged to enable patterned light delivery. In combination, arrays of LED-coupled optical fibres can enable patterned light delivery to deep targets in the brain. Here the authors describe the process flow for making LED arrays and LED-coupled optical fibre arrays, explaining key optical, electrical, thermal and mechanical design principles to enable the manufacturing, assembly and testing of such multi-site targetable optical devices. They also explore accessory strategies such as surgical automation approaches as well as innovations to enable low-noise concurrent electrophysiology.

1 Introduction

Optogenetics has been widely applied to the control of single or small numbers of deep structures in the brain (e.g. using a fibre-coupled laser [1–4]), as well as to patterned control of superficial brain areas (e.g. using scanning lasers, light-emitting diode (LED) arrays and other two-dimensional (2D) patterning strategies (e.g. [5–7]). Recently, we have engaged in developing devices that exhibit both the scalability to high target counts exhibited by 2D arrays of light sources, and the deep structure targetability of optical fibres, by delivering the light from a 2D array of custom-placed sub-millimetre-sized LEDs, into a set of custom-length optical fibres that are individually docked to LEDs [8, 9], even in wireless fashion [10]. A key advantage of this methodology is that these devices can be built and tested by individual groups using simple machining and assembly techniques. We here present the process for design and construction of LED arrays and LED-coupled optical fibre arrays, demonstrating the key engineering principles of design and fabrication.

Such devices are compact and lightweight, and are easily carried by freely moving mice. Our design is centred around a procedure in which a 2D LED array is assembled, and a set of custom-length fibres are docked to it, in a single step, thus enabling easy end-user customisation and fabrication of a set of arrays in a matter of days, using inexpensive computer-based automated machining tools. We enable device operation for behaviourally relevant timescales, and can support electrophysiological recording concurrent with optical illumination. We describe new tools to systematise the surgery, facilitating good device insertion.

2 Materials and methods

2.1 LED and fibre-coupled LED array fabrication: design and preparation of key structural components

Fibre arrays are made of an array of optical fibres (components '1' in Fig. 1*a*), which are docked to a planar set of LEDs (components '2' in Fig. 1*a*). The alignment of the fibres to LEDs is achieved via a stack of structural components (the fibre alignment plate, reflector plate and LED base plate, components '5', '7' and '11' in Fig. 1*a*, respectively) that hold the optical elements (LEDs and optical fibres) in precise positions (within 10 µm) relative to guide holes on the structural components. The guide holes are aligned with device assembly guideposts (component '8' in Fig. 1*a*) to hold the stack of structural components in the proper position. Detailed assembly instructions are given in the following sections, and the purpose of each component is explained in Section 3.1.

To facilitate the design and creation of fibre arrays, we developed a pipeline of computer-aided design and fabrication tools. We use EAGLE, a free CAD programme, to graphically lay out all of the components in the fibre array (see 'Supplementary Figure S1' for a schematic of the hippocampal CA1-targeted fibre array in EAGLE), and we use a tabletop, computer-controlled mill (MDX-15, from Roland DGA) to cut components '5', '7', '10' and '11' (see Fig. 1*a*) out of stock materials. MATLAB scripts act as a bridge between the design and fabrication processes, translating specifications for the arrays extracted from EAGLE into machine code readable by the mill. Crucially, EAGLE provides methods for automated data input, through script files, as well as automated data output, through its CAM processor. Thus, array specifications stored in a MATLAB script can be visualised and then adjusted in EAGLE, and changes made in EAGLE can be recorded in the MATLAB script. Details are provided in section 'S3. Supplementary Methods: Fibre Array Design Guide'.

2.2 Fibre array fabrication: preparation of other components

A number of other components must be prepared prior to assembly into a fibre array. Optical fibres (component '1' in Fig. 1*a*) are prepared from 0.48 NA, 200 µm-diameter core optical fibre (Thorlabs) by sectioning into 1 in-long segments with a razor blade and removing all jacketing with a wire stripper (Stripmaster). To facilitate reliable and repeated cleaving of fibres to desired length, a diamond fibre cleaver is used, in conjunction with fibre length trimming shims (milled according to the instructions in 'Supplementary Methods S3.4 Computer-Aided Fabrication of Other Fibre Array Components'), which are small blocks that fit in a slot of the diamond cleaver and are milled to the length of each fibre. The fibre segment is inserted into a diamond fibre cleaver (Delaware Diamond Knives) against the back of the cleaver, and cleaved once. The fibre is then pushed forwards within the cleaver the length of the shim of desired fibre length (i.e. by placing the shim between the fibre and the back of the cleaver), and cleaved again, producing an optical fibre the length of the shim with optically

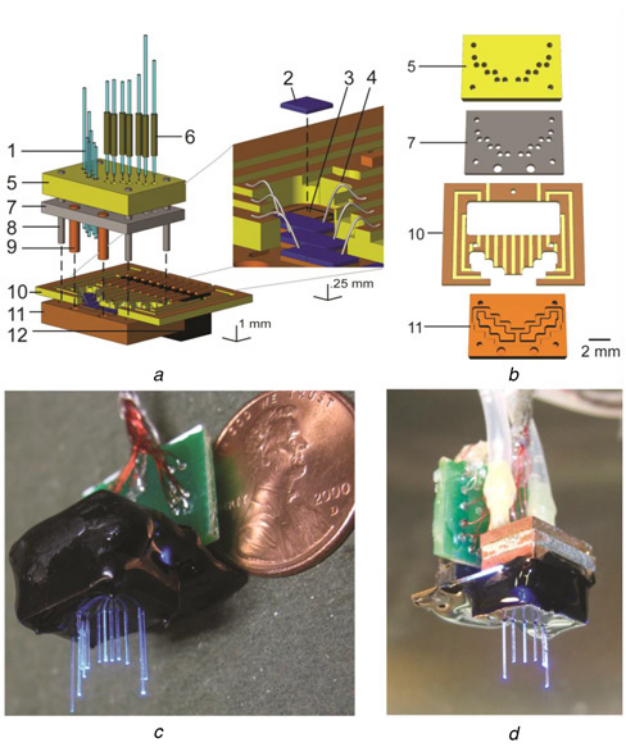

Fig. 1 *Design and fabrication of optical fibre arrays*
a Schematic, in exploded view, of a fibre array with fibres pointing upwards, with 'inset' zoomed in on LEDs and their connections, adapted from [8] to [10]
Vertical dashed lines denote points at which components dock together when the device is assembled
Numbers refer to key components: 1, optical fibre; 2, LED; 3, LED pedestal (carved out of LED base plate, 11); 4, wire bond; 5, fibre alignment plate; 6, fibre fitting; 7, reflector plate; 8, device assembly guidepost (to be removed after final assembly, but before implantation); 9, reflector plate heat conduit; 10, circuit board; 11, LED base plate; and 12, circuit board connector
b Key structural components, numbered the same as in A
c Photograph of a relatively dense hippocampal CA1-targeted fibre array device (schematised in A), appropriate for silencing the entire hippocampus for example, with fibres pointing downwards, with a penny for scale
d An 8-fibre hippocampal array, appropriate for stimulating multiple points in the hippocampus, shown with optional cooling module before encapsulation with biocompatible epoxy

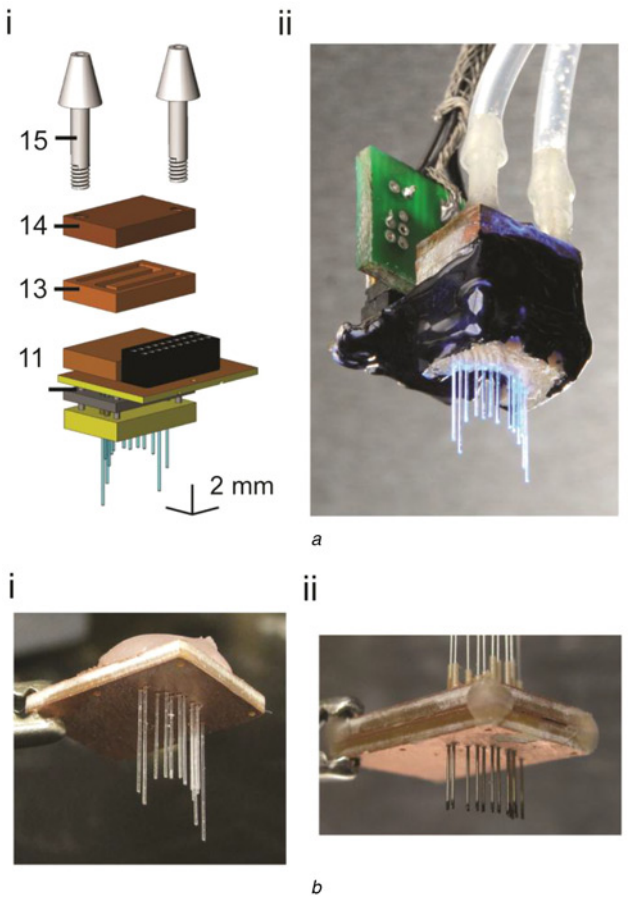

Fig. 2 *Accessory devices, and modifications, for implantation and utilisation of fibre arrays*
a Fluidic cooling system, added to the back of the fibre array, appropriate for increasing the amount of time the array can be run continuously. (i) Schematic, in exploded view, of the cooling system, added to the back of the fibre array. Numbers refer to key components: 11, LED base plate; 13, fluidic cooling channel plate; 14, fluidic cooling channel backing plate; and 15, barbed fluidic connector. (ii) Photograph of a cooled hippocampal CA1-targeted fibre array (based on the design in Fig. 3*a*i)
b Accessory devices to aid fibre array implantation. (i) Practice array, with the same targets as the array schematised in Fig. 2*a*, shown during fabrication before encapsulation with biocompatible epoxy. (ii) Parallelised craniotomy marker, consisting of freely moving hypodermic steel tubing with inked tips, appropriate for conforming to the contours of the skull and marking sites of craniotomies for fibres

smooth cleaves on both ends. This process is repeated for each desired fibre.

Guide posts (component '8' in Fig. 1*a*) are made of 0.020 in stainless steel wire (small parts), cut into 1 cm lengths (e.g. using a Dremel abrasive wheel). Heat conduits (component '9' in Fig. 1*a*) are made of 1/32 in copper wire (McMaster-Carr), cut into 3 mm lengths.

When fluidic cooling is used, cooling channels and backing plates (components '13' and '14' in Fig. 2*a*i) are cut from 1/16 in thick copper plates with waterjet cutters, and holes in the backing plates are threaded with a 0–80 tap. Fluidic barb connectors (component '15' in Fig. 2*a*i) are 3D printed, and the ends are threaded with a 0–80 die.

2.3 *Fibre array fabrication: assembly*

The first set of steps of device assembly is to put the LEDs and the circuit board (components '2' and '10' in Fig. 1*a*) onto the LED base plate (component '11' in Fig. 1*a*). The LED pedestals (component '3' in Fig. 1*a*) are pre-tinned by depositing a thin layer of solder paste on top and then heating the LED base plates on a hot plate set to 235°C for 20 s. Then additional solder paste, as well as raw die LEDs (e.g. Cree EZBright Gen II EZ500, EZ600, EZ700 or EZ1000 chips), are put on the pedestals. At this time, we also place the circuit board (component '10' in Fig. 1*a*) atop the LED base plate, with a thin sandwich of solder paste in between. The device assembly guideposts (component '8' in Fig. 1*a*) are then inserted through the guidepost holes so as to align the circuit board to the LED base plate. Optionally, the fluidic cooling channel plate (component '13' in Fig. 2*a*) and fluidic cooling channel backing plate (component '14' in Fig. 2*a*) are attached to the LED base plate with solder paste, forming a water-tight seal. This assembly is heated on the hot plate for another 20 s, during which LEDs self-align to the edges of the pedestals because of the surface tension of the liquid solder. Guideposts are removed after the device has cooled. The electrical connector (component '12' in Fig. 1*a*) (i.e. Samtec FTE10) is then soldered to the circuit board. A copper wire is inserted through the via (the top hole in the circuit board, Fig. 1*b*) and soldered to both sides of the circuit board; this connects the positive voltage supply, coming from the electrical connector on the top side of the circuit board to the plane of copper on the bottom side of the circuit

board and the LED base plate, which provides the positive voltage source common to all the LEDs soldered onto the LED base plate. Finally, the assembled apparatus is cleaned of flux residue in a small plastic tube filled with isopropyl alcohol inside an ultrasonic bath.

The assembled apparatus is next hot glued to a glass slide with the coolant backing plate (for cooled arrays) or LED base plate (for uncooled arrays) flat against the slide. LED bond pads are wedge bonded to copper circuit board traces via 0.001 in aluminium wire (using a wire bonder, West Bond 747677E-79C).

The remainder of the key structural parts, the alignment plate and the reflector plate (components '5' and '7' in Fig. 1*a*), are linked by the four device assembly guideposts, and epoxied around the edges to insure a small (e.g. 1 mm) gap for thermal insulation. Reflector plate heat conduits are inserted into the reflector plate and attached with thermal epoxy. Fibre fittings (component '6' in Fig. 1, made from PEEK tubing 0.010 in inner diameter, 0.018 in outer diameter for the plates as designed above) are inserted through the alignment plate and reflector plate and cut flush with a razor blade on both sides, then set in place by filling the space between the alignment plate and reflector plate with epoxy. Then the optical fibres are loaded into the polyether ether ketone (PEEK) fibre fittings. This second assembly is then lowered onto the LED base plate so that the guideposts insert into the guidepost holes of the LED base plate, and the optical fibres are just above (~100 µm) the LEDs. Optics glue (Thorlabs) is then applied to the LED-fibre interface and cured with a ultraviolet lamp. The reflector plate heat conduits are bonded to the LED base plate with thermally conductive epoxy. The spaces in between the reflector plate, the circuit board and the LED base plate are filled with 5 min epoxy, and after curing, the guide posts are rotated about their own axes gently to loosen them from the epoxy, then pulled out of the device. To seal the outside of the device to insure biocompatibility, to prevent electrical shorts and to block stray light from emitting, the exposed leads of the electrical connector are sealed with hot glue, and the surface of the device is coated with black epoxy. Finished arrays are released from the glass slides by placing the slides on a hot plate at 100°C until the hot glue attaching the array to the slide (described in the previous paragraph) becomes soft (this procedure does not affect the hot glue used to seal the exposed leads of the electrical connector). Finally, if cooling is used, barbed fluidic connectors (component '15' in Fig. 2*a*, 3D printed out of acrylic and threaded on the outside with a 0–80 die) are screwed into the holes in the coolant backing plate and sealed to the plate with epoxy.

For the bilateral CA1 14-fibre design (Figs. 1*a*–*c*), we chose fibre termini (listed in the following list, in units of millimetres anterior, lateral and ventral to bregma) of: (−1.7, ±0.6, 1.25), (−1.7, ±1.3, 1), (−2.4, ±1.5, 0.9), (−2.4, ±2.2, 1.1), (−3.1, ±4.1, 4.25), (−3.1, ±2.5, 1.2) and (−3.8, ±3.85, 2.75), so that 14 LEDs were used with centred fibres; arrays were constructed both with and without cooling modules.

2.4 *LED driver circuit design and operation*

The LEDs can be controlled using a standard LED driver circuit with a transistor and current-limiting resistor connected to the cathode of each LED. Importantly, the anodes of the LEDs are all connected together on the LED base plate, and it is desirable to tie the LED base plate to earth ground. Therefore the LED cathodes must be connected to a negative voltage supply. We built a custom circuit board to facilitate controlling the LEDs with ground-referenced digital logic signals ('Supplementary Figure S4' and 'Supplementary Figure S5').

2.5 *Fibre array testing: light power*

We measured light power output with $n = 7$ Cree EZ600 LEDs, each coupled to a 200 µm core-diameter, 0.48 numerical aperture (NA) optical fibre. Power measurements were performed with an integrating sphere photometer (Thorlabs). Arrays were fit in place over the integrating sphere (with original connector removed) with a lasercut adapter with a dock for the alignment plate, which blocked stray light from entering from the integrating sphere. Individual LEDs were run at 500 mA with water cooling (room temperature, 30 ml/min, with a peristaltic pump) for several seconds to obtain a stable measurement. Measured power was divided by optical fibre tip surface area to obtain irradiance.

2.6 *Fibre array testing: thermal testing in vivo*

We measured temperature within the dental cement between a fibre array and the skull of a mouse (an acute experiment under isoflurane anaesthesia, body temperature maintained with a heating pad). We

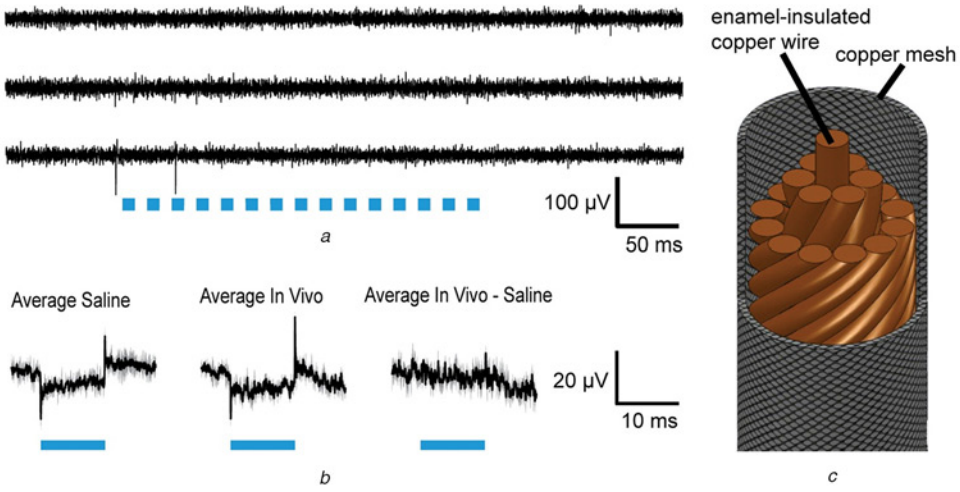

Fig. 3 *A custom coaxial cable design enables decoupled LED activation and recording*
a Raw traces of three electrode recordings on a tetrode (the fourth electrode here acts as amplifier reference), of neurons in the cortex of an awake headfixed mouse (non-ChR2-expressing) during 50 Hz LED operation (each pulse was for 10 ms at 500 mA, indicated by blue bars)
b Average, across trials and electrodes, of 33 traces obtained in each of the saline ('left') and in vivo ('middle') conditions, displayed as mean (solid lines) ± standard deviation between electrodes (shaded area). 'Right', average of the 33 traces obtained in vivo, after each trace was preprocessed by subtracting off the saline-characterised artefact recorded on the same electrode (and averaged across all trials for that electrode, e.g. 11 trials)
c Schematic of the 'spatially averaged' multichannel coaxial cable utilised to deliver power to LEDs while minimising capacitive and inductive coupling to recording electrodes

tested two cooled hippocampal arrays (room temperature water coolant circulated through the cooling module with a peristaltic pump, 30 ml/min) and two uncooled arrays with two LEDs each, in each case with a disposable thermistor (Digikey part 495-2159-ND) embedded in the dental acrylic between the array and the skull. The thermistor was placed in a voltage divider circuit, and the thermistor voltage acquired by an NI-DAQ board, digitised at 10 Hz. We sampled the space of fibre array powers and fibre array durations of operation over a wide range of protocols of interest to neuroscientists. To facilitate further extrapolation to protocols not explicitly tested here, we additionally performed a curve fit for each of the two datasets (the cooled array dataset and the uncooled array set), modelling the system as undergoing two processes: fast-timescale dumping of heat into the system and slower-timescale heat dissipation to the environment. A convenient approximation to these two guiding principles is simply to fit the empirical data with a two parameter equation that both captures the kinetics of heat generation and of heat dissipation; to first order, this can be written as

$$T = a^*P^*D/(1 + b^*D)$$

expressing temperature increase, T, as a function of the total fibre array power (as utilised in Fig. 3*a*), P, as the duration of fibre array operation, D and two free parameters, a and b.

2.7 Fibre array fabrication: optimisation for electrophysiology

Two sets of cables are needed for joint optical fibre array perturbation with concurrent recording: one to carry power to the LEDs and one to carry neural signals back (for this, a conventional cable is fine). For the power cables, we developed a novel style of coaxial cable (Fig. 3*c*), which is designed to eliminate inductive and capacitive coupling to nearby surfaces and wires. Briefly, the outside comprises a tubular copper mesh (Daburn), held at ground (which eliminates capacitive coupling), that provides a current path from a power supply to the common anode of the LEDs; running inside the mesh is a bundle of twisted copper strands (33 gauge magnet wire, MWS Industries, twisted with a power drill) that serve as individual current return paths for each LED's cathode. For the internal copper wires, determining how the pins of the two male connectors correspond can be accomplished with a multimeter. Importantly, the helical copper strands and the tubular copper mesh are coaxial and carry equal and opposite currents, minimising the inductive coupling between the cable and nearby recording devices.

2.8 Electrophysiological recording and data analysis

We performed acute cortical recordings in an awake, headfixed mouse, using an LED-coupled fibre with a tetrode epoxied to the side of the fibre. To prevent photoelectrochemical artefacts [3, 11] from corrupting our measurement, during the construction of the device a thin opaque FR1 plate was placed between the LED and the end of the fibre. Neural signals were amplified 20× by a headstage amplifier and 50× by a second stage amplifier (Plexon), digitised at 30 kHz with a Digidata (Molecular Devices) and analysed with pClamp and MATLAB. After neural recordings were established, LEDs were then driven at 500 mA for 10 ms pulse durations at 50 Hz for 300 ms train durations (i.e. 15 pulse repetitions), with a pulse train every 5 s, for 1 min sessions. The same measurements were repeated with the tetrode and fibre tips in saline. For analysis of LED–electrode coupling, we analysed the data obtained from 11 LED pulses that were delivered at 10 ms duration at maximum power, after at least 50 ms of darkness (three electrodes, for a total of 33 total traces). We calculated average and standard deviation traces in MATLAB, aligning traces on the LED pulses. We computed the difference between the neural and saline artefacts by subtracting the averaged saline artefact from each raw neural trace, and then averaging the resultant subtracted neural traces. To look for action potentials, traces were bandpass filtered between 270 and 8000 Hz.

2.9 Fibre array fabrication: accessories for surgery practice and surgery facilitation

Molds for assembling practice arrays (see 'Supplementary Figure S2' for a picture of mold during assembly) are created from 1/16 in FR1 epoxy laminate plates, each plate of which is milled separately (see 'Supplementary Methods S3.4' for details on milling), and which are then stacked on top of each other, aligned with guideposts that go through holes milled in each of the four corners (and that stick out, for use in practice array assembly). Plates are secured to each other on the sides with hot glue. The key design feature of the practice array assembly mold, facilitated by the computer-aided design and fabrication system, is that each component plate is milled to have holes that line up, in the final stacked assembly, to form columns through which fibres can be inserted, so that each fibre is immersed in the mold to a depth which equals its ultimate desired depth in the brain. To enable fibres to be inserted into these columns so that the centres of the fibres are precisely aligned, pieces of PEEK tubing (i.e. identical to the PEEK fibre fitting utilised above, component '6' in Fig. 1*A*) are inserted into the plates as described in the above section; to facilitate replacement of PEEK tubing (e.g. if damaged) without having to remake the whole practice array mold, the PEEK tubing pieces can be mechanically constrained (e.g. by being inserted into a plate that is flanked above and below by plates with smaller holes than the outer diameter of the PEEK tubing).

Practice arrays (Fig. 2*B*i) are constructed by placing a practice array plate (essentially a fibre alignment plate, with holes drilled where the fibres pass through, with an extra tab sticking out, to facilitate later attachment of an electrical connector to enable mounting on the stereotaxic arm; see 'Supplemental Methods S3.4' for details) over the practice array assembly mold, so that the guideposts pass through the guidepost holes in the practice array plate. Then, PEEK fibre fittings (component **6** in Fig. 1*a*) are inserted into the holes in the practice array plate, and trimmed to the thickness of the plate. Optical fibres are stripped of their jacketing and inserted through the PEEK fibre fittings in the practice array plate, down into the practice array assembly mold until the fibres touch the bottoms of the columns that have been machined to insure that the appropriate lengths of fibre extends below the end of the practice array plate. Optical fibres are cut so that a few millimetres of fibre extend above the practice plate, and then hot glue is placed on top to hold the fibres and PEEK fittings to each other and to the plate. An electrical connector (identical to component '12' in Fig. 1*a*) is epoxied onto the top of the practice plate, to help with later holding by the stereotax during surgery. The practice array plate is encapsulated in biocompatible epoxy.

Parallelised craniotomy markers (Fig. 2*b*ii), to aid in the stereotactic determination of coordinates for drilling craniotomies to insert fibre arrays into the brain, are constructed by supergluing PEEK fibre fittings into the holes of a practice array plate (see above and 'Supplementary Table S1'). Hypodermic tubing (32 gauge, ~1 cm long) is cut and then inserted into the PEEK fibre fittings. An electrical connector (identical to component '12' in Fig. 1*a*) is epoxied onto the top of the automated craniotomy marker, to help with later holding by the stereotax during surgery.

2.10 Fibre array implantation

All animal procedures were in accordance with the National Institutes of Health Guide for the care and use of Laboratory Animals and approved by the Massachusetts Institute of Technology Animal Care and Use Committee. Mice were anesthetised with isoflurane in oxygen, and then administered buprenorphine and meloxicam for analgesia. After revealing the skull, and

doi: 10.1049/joe.2014.0304

levelling bregma and lambda to the same vertical position, the sites for craniotomy opening were indicated by using a parallelised craniotomy marker (essentially an alignment plate with freely moving hypodermic tubing inserted within, and dipped into sterile, biocompatible ink, see Section 2.9 for details) held by the stereotax and lowered, to mark the locations of all the drill sites in one step. Then three small screws (size 000, 3/32 in long, J.I. Morriss) were implanted to make a broad-based tripod for attachment of the fibre array atop the skull [12]. Small craniotomies in the skull were made, over each ink-stained drill site, with a hand drill (e.g. Barrett pin vise, with HSD-75 drill bit); alternatively, a large craniotomy was made around the outline of the ink-stained drill sites with a dental drill. Then, the optical fibre array to be implanted was attached to a custom holder (essentially a Samtec connector on a post that plugged into the electrical connector of the fibre array, component '12' in Fig. 1*a*), and then lowered using a stereotaxic apparatus (e.g. Kopf) so that the tips of the optical fibres were 250 µm above the target coordinates, as explained above. Then, the fibre array was secured to the three skull screws with dental acrylic; it is important to 'loop' the wet acrylic over the array to mechanically secure everything together.

3 Results

3.1 Fibre array design, fabrication and operation

We have previously shown that arrays of LEDs, patterned on a substrate to match the shape of target brain regions and implanted above the surface of the cortex, can be used to control behaviour with optogenetic stimulation [10]. These arrays, wirelessly controlled and powered, allow a freedom of movement impossible to achieve with optical stimulators tethered to distal lasers. Additionally, the method used to pattern the LEDs on the substrate achieves a packing density (<1 mm centre-to-centre) and precision (features to mount LEDs machined with 25 µm resolution) that would be extremely difficult to achieve with traditional stereotaxic methods of implanting individual optical fibres. Thus, we sought to develop a method for fabricating arrays of optical fibres to be coupled to our arrays of LEDs, in order to target deep brain structures with the same precision we have employed to target surface structures.

One core innovation used here is an efficient, precise way of docking a large set of optical fibres to a large set of LEDs arrayed on a planar surface, so that the resultant device can safely and effectively deliver light independently to a set of sites distributed in a 3D fashion in the mammalian brain (Fig. 1). We chose our fibre-LED coupling strategy to maximise light output from an optical fibre of fixed width, using optical fibres with high numerical aperture LEDs with high surface irradiance. According to a theorem derived in [13], maximal light coupling from an LED into an optical fibre is achieved when a fibre is in direct contact with an LED, and the surface area of the LED is greater than the fibre. This coupling method simplifies device design by removing the need for additional optics, and the Lambertian emission pattern of LEDs tolerates alignment errors of several degrees thanks to the angle-independent irradiance of LEDs, in contrast to lasers which must be precisely aligned.

Using this coupling method, placement of a 200 µm optical fibre (0.48 NA) onto a 600 µm × 600 µm LED (465 nm wavelength Cree EZBright600), with the small gap bridged by an index-matched adhesive (see Section 2.3), yielded a maximum irradiance at the free end of the fibre of 220 ± 10 mW/mm^2 (mean ± standard deviation; LED run at the less-than-maximal current of 500 mA; $n = 7$ LED-coupled fibres, using the testing procedure described in Section 2.5), matching fibre tip irradiances commonly used in vivo for safe illumination of opsin-bearing cells [1–3]. At this tip irradiance, a fibre can illuminate the edges of a >1 mm^3 volume to an irradiance of >1 mW/mm^2 (as reflected by computational models and experiments in [1, 2, 14]), a light level at which many commonly used microbial opsins are significantly activated [14–17]. Thus, depending on the scientific goal at hand, LED-coupled fibres can be packed together to guarantee 'tiling' of brain structures (~750 µm apart, as in Figs. 1*a–c*, a 'dense' bilateral CA1 hippocampus targeting array) or spaced sparsely (~1.5 mm apart, as in Fig. 1*d*, a 'sparse' bilateral CA1 hippocampus targeting array). Detailed guidelines on how to lay out the geometry of such fibre arrays, optimising LED and fibre placement are provided in 'Supplementary Methods S3.1 Choosing Coordinates for Fibre Arrays'.

To fabricate a 3D fibre array, we first fabricate a 2D array of LEDs, using computer-aided circuit design and manufacturing tools, and then align and dock the set of optical fibres to the set of LEDs, in a single positioning step. We here describe the principles of the design; detailed step-by-step instructions for semi-automatically manufacturing the components and performing the assembly are given in 'Sections 2.1-3 Fibre Array Fabrication' and 'Supplementary Methods S3.3 Computer-Aided Fabrication of Key Structural Components'. Notably, only two relatively inexpensive machines not commonly found in an ordinary neurophysiology laboratory are required, a tabletop mill and a wirebonder. Assembly proceeds in two phases: in the first phase of construction, raw die LEDs (component '2' in Fig. 1*a*) self-align onto solder-coated planar pedestals (component '3') to form a 2D array of LEDs on a copper LED base plate (component '11'), and then LED terminals are wirebonded (component '4') to an attached circuit board (component '10'); the circuit board bears copper traces for provision of power to individual LEDs, and a connector to connect the LED array to the outside world (component '12'). In the second phase of construction, an alignment plate (component '5') and reflector plate (component '7') that firmly hold, via fitted pieces of tubing (component '6'), a set of optical fibres (component '1') cleaved to lengths that correspond to the dorsoventral coordinates of brain targets, is then lowered onto the 2D LED array along a set of assembly guideposts (component '8'); optical adhesive is used to couple fibres to their corresponding LEDs. The reflector plate is then thermally connected to the LED base plate via copper heat conduits (component '9'). Finally, exposed surfaces of the device are coated with biocompatible epoxy. For surgical practice, fibre arrays without LEDs can be very rapidly fabricated, as shown in Fig. 2*bi* and Supplementary Figure 2, and described in Section 2.9 and 'Supplementary Methods S3.4'.

Several key mechanical, optical and electrical engineering innovations equip the device with the properties of easy end-user design and fabrication, good optical performance, compact size and small weight, good thermal management and low electrical noise production. For example, after brain targets are chosen by the user, the four key structural plates (components '5', '7', '10' and '11' in Fig. 1*a*) are all semi-automatically machined out of their respective materials by a tabletop mill, which is controlled by a PC that runs custom scripts (e.g. in MATLAB) that convert LED coordinates into mill instructions (see 'Supplementary Methods S3.3 Computer-Aided Fabrication of Key Structural Components' for details). Precision machining of all core structural plates from a single set of parameters insures high precision of fibre location along medio-lateral and anterior–posterior axes (<10 µm variability). To ensure a similar precision for the positioning of small raw LED dies onto the LED base plate, we utilised a self-alignment strategy in which the surface tension of solder on the LED pedestals (component '3' in Fig. 1*a*) automatically positions the LEDs in the proper geometry. Once assembled, such a device occupies <0.5 cm^3 in volume, and weighs <1 g, and thus is easily carried by a freely moving mouse on its head.

To achieve the compactness of our device, we use the LED base plate (component '11' in Fig. 1*a*) as not only the mechanical LED mount and heat sink, but also as the common anode for all the LEDs. To power LEDs wired in this way, we designed a custom LED driver circuit board to receive TTL pulses (from any

commodity source, e.g. an NI-DAQ board) and then to trigger the board to transmit the appropriate power to control the LEDs (see Section 2.4 for a description of the circuit, 'Supplementary Figure S3' and 'Supplementary Figure S4' for a schematic and layout of the LED driver circuit). We designed a novel geometry for a multichannel coaxial cable (visible in Figs. 2*c* and *d*, and schematised in Fig. 3*b*) to provide power to the LEDs on the fibre array; this cable uniquely minimises both capacitive and inductive coupling of electrical signals to nearby structures (e.g. recording electrodes, Fig. 3*a*) while allowing for dozens of independent current-carrying LED control lines in a flexible cable format; this cable is described in more detail in Section 2.4. We use pulleys and a counterweight to offset the weight of the electrical cable (and, optionally, of the cooling tubing, described below) that enables practically free mouse movement (and could be used in conjunction with electrical and fluidic commutators, if necessary).

Thermal management is an important consideration for these devices because our optical coupling strategy, chosen to maximise the light output from optical fibres, has a tradeoff in power efficiency. There are two causes for this. As the drive current to an LED increases, its efficiency (measured in light output power over electrical input power) decreases. We chose to use a 500 mA drive current, which is near the knee of the power efficiency curve. The second efficiency loss is because of the optics governing the coupling of LED light to an optical fibre – by using an LED larger than the optical fibre, we make sure to fill the surface of the fibre with light, but also create a lot of light beyond the edges of the fibre which cannot be coupled in. Ultimately, we use almost 2 W of electrical power to generate roughly 300 mW of light power, of which 7 mW is coupled into an optical fibre.

We designed the LED base plate to function as a high heat-capacity heat sink to pull heat away from the mouse skull. Since the LEDs are soldered directly to this heat sink, heat that is generated during light production has a very low resistance path into the heat sink. To account for optical energy that is not coupled into the fibres, we chose to direct light power away from the head and back towards the heatsink with a highly reflective aluminium reflector plate (component 7) attached to the fibre alignment plate with thermally insulating epoxy. Aluminium absorbs much less blue light than copper, and calculations indicate that this strategy reduces the heat delivered towards the skull by stray LED light by approximately two orders of magnitude, against a design without a reflector.

To determine the safe operating regime for a fibre array, we devised an experiment to measure the temperature that would occur near the skull of mouse with an implanted fibre array during fibre array operation. We determined that for a conservative restriction of 1°C temperature increase, the heatsink could absorb 7 s worth of LED operation, which may be distributed over longer time periods (e.g. running one LED for 14 s at 50% duty cycle) or divided among multiple LEDs (e.g. running ten LEDs for 0.7 s). To expand the range of fibre array protocols of operation possible, we devised a supplementary cooling module (shown in Fig. 2*a*) that increases the maximum amount of energy that can be consumed on the device by an order of magnitude or more (dotted lines and filled diamonds in Fig. 4). In this modified design, a microfluidic cooling channel plate (component '13', with microfluidic cooling channel backing plate, component '14', in Fig. 2*ai*) attaches to the back of the LED base plate to support water cooling of the device (via connectors, component '15' in Fig. 2*ai*, that connect to tubing that leads to a peristaltic pump). A modest cooling system (using 750 µm diameter channels and room temperature water flowing at a constant rate of 0.5 ml/s) enables a ∼9× increase in the duration of the protocol of operation for one LED or a ∼5× increase in the duration of the protocol of operation for ten LEDs. After the fibre array is run on a protocol of operation, the array cools to baseline temperature with a time constant of 3.8 ± 0.1 min (mean ± standard deviation; $n = 2$ arrays), meaning that the available 7000 LED-ms of device operation can be re-utilised every few minutes, appropriate for many behavioural paradigms. Note that if a fibre array protocol of operation involves slow heat generation compared with this time constant – that is, the LEDs are run at a low-power level or the LEDs are pulsed at a very low frequency, then such a protocol of operation can continue indefinitely (Fig. 4, steep upper left part of each curve). Additionally, the time constant of array cooling speeds up to just 1.5 ± 0.5 min (measured for $n = 2$ arrays).

3.2 Implantation, utilisation and validation of fibre arrays in behaving mice

Surgical implantation of fibre arrays into the mouse brain takes place under anaesthesia, after the insertion of three anchor screws into the skull [12]. We have begun the process of automating the surgery; for example, we mark all of the craniotomy sites needed for fibre array insertion in a single step by lowering onto the skull an array of free-sliding micro-pens so that each marks the location of a craniotomy with an ink dot (see Fig. 3*b*ii and Section 2.9).

3.3 Integration of electrophysiological recording and fibre array illumination

The fast pulses of current that power the LEDs of a fibre array can potentially result in artefacts on nearby conductors via capacitive and inductive coupling. To solve this problem, we developed a lightweight multichannel coaxial cable to convey power to the LEDs (schematised in Fig. 3*c*). The key design innovation is to have the internal wires of the cable spiral about the central axis of the cable, so that as seen from outside the cable, each individual internal wire spatially averages so as to simulate a true coaxial cable, in conjunction with an outer copper mesh. Currents (500 mA and 10 ms long) delivered to an LED on an array resulted in little noise on electrodes running along the corresponding fibre on the array. The small, low-frequency artefacts that did couple in (average peak of 15 ± 4 µV, avg ± standard deviation across electrodes, $n = 3$ electrodes) were identical between recordings performed in saline and in vivo, enabling high-fidelity subtraction, leaving undetectable noise (Fig. 3*b*).

4 Discussion

We here present the design and fabrication methodology for a device that comprises an array of custom-length optical fibres docked to a 2D array of LEDs [8–10], which enable independent light delivery to sites distributed in a 3D pattern throughout the mammalian brain, important for targeting realistically shaped brain circuits for neural perturbation. Our device possesses a form factor that is compact and lightweight enough (e.g. ∼1 g, ∼0.5 cm^3) to be borne by freely moving mice. Each individual fibre can easily address a volume on the order of a cubic millimetre with irradiances on the order of 1 mW/mm^2; greater volumes are addressable at lower light powers. The device can be operated for periods of time appropriate for many behavioural experiments; when used in conjunction with a supplementary fluidic cooling apparatus, it can support experiments in which large numbers of LEDs are operated for long durations. For power delivery, our device utilises a novel multichannel coaxial cable, which minimises capacitive and inductive artefacts on adjacent neural recording electrodes. Finally, we devised new tools to systematise surgery, enabling large numbers of fibres to be inserted through targeted craniotomies. We demonstrate how to build these devices using just two inexpensive manufacturing devices in addition to what might be found in a modern neurophysiology laboratory. With some practice, creating a batch of fibre arrays, from design to final assembly, takes just a few days. Building devices in the laboratory is advantageous

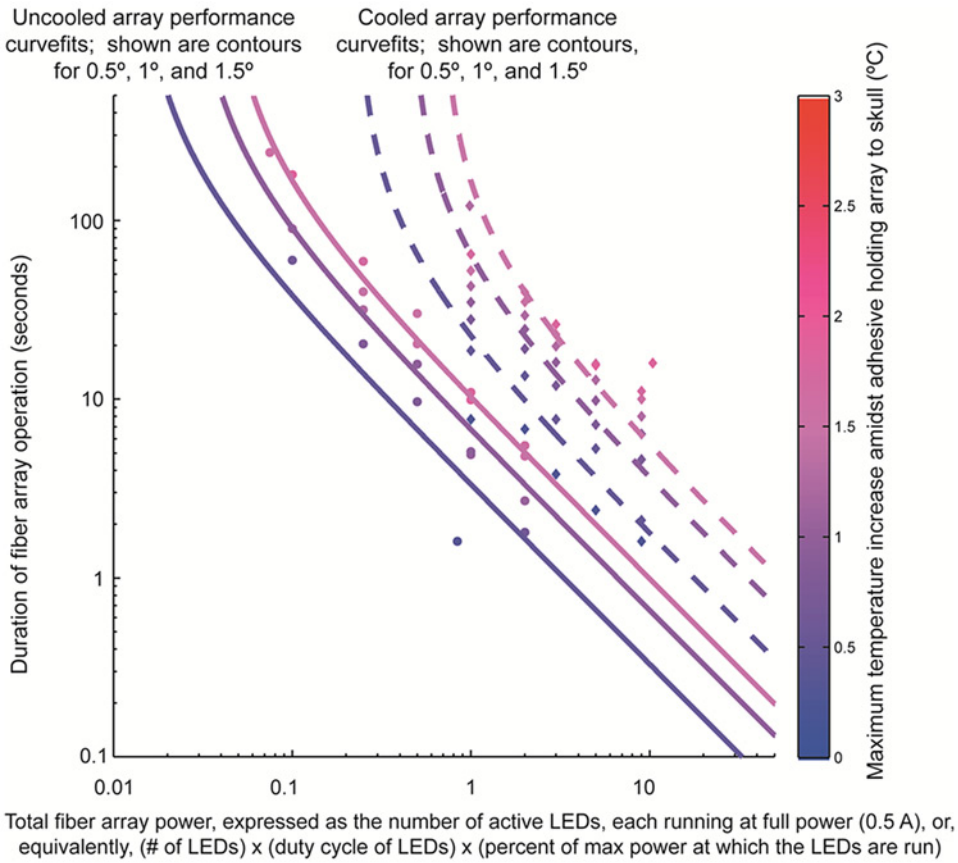

Fig. 4 *Thermal characteristics of fibre array use*
Maximum temperature increase at a point in the material (dental acrylic) holding an array to the skull of an anaesthetised mouse, for uncooled (solid lines, circles, $n = 2$ arrays) or cooled (dotted lines, diamonds, $n = 2$ arrays) fibre arrays, plotted as a function of the total fibre array power (x-axis, expressed in units of the number of active LEDs running at 500 mA) and the duration of fibre array operation at that given total fibre array power (y-axis). Shown for clarity is the behaviourally relevant portion of the temperature increase dataset acquired (circles and diamonds), as well as mathematically fit isothermal contours of temperature increase by 0.5, 1 and 1.5°C

for rapid prototyping when designs may change often, but fabrication and assembly could also be outsourced. The maturation of 3D printers may also soon offer sufficient resolution to simplify many parts of the fabrication process.

To simultaneously achieve in a single device the many specifications required – 3D targeting of light with good optical performance, easy end-user design and fabrication, compact size and small weight, low heating and electrical noise – required a large number of optical, mechanical, electrical and thermal variables to be simultaneously optimised. For example, the coupling strategy between LEDs and fibres not only maximises light throughput, but also enables single-step alignment of a large number of optical fibres to a 2D LED array. The core structural plates of the device enable not only this single-step alignment process, but also provide for heat management, and support passive electrical noise cancellation.

Some performance tradeoff decisions are required when specifying the device design. Although our light-coupling strategy maximises light output from our optical fibres, it sacrifices overall power efficiency – 3% of the light output from an 600 µm LED is coupled into a 200 µm optical fibre – which also places demands on thermal management for the devices. Efficiency could be increased by decreasing LED size (decreasing overall fibre output power and increasing power output variability between fibres because of manufacturing tolerances) or using laser diodes instead of LEDs (increasing device complexity). Thermal management could be extended to support many more LEDs with the use of low-temperature fluids for array cooling, in conjunction with active thermistor feedback. Thus, with different choices for what parameters to optimise, the design principles for these arrays can be used to support applications with many different kinds of constraints. There are also many possibilities for how these fibre arrays may be customised and augmented. Our device uses blue LEDs, appropriate for activation of not only opsins whose action spectra peak in the blue such as ChR2, Mac and Chronos [18], but also many other opsins such as Arch that have action spectra peaks in the green or yellow, but are also well activated by blue light. In the case of Arch, for example, its sensitivity to light at 470 nm is ~50% of its peak sensitivity, still enabling very significant silencing in a region [14]. Other colours of LEDs may also be used, such as high-power 625 nm LEDs to drive the red-light sensitive silencer Jaws [19]. We expect that as consumer applications drive improvements in the components that make up the fibre array – for example, LEDs become more efficient, digital fabrication becomes cheaper – the fibre array device itself will ride these technology development curves, becoming more powerful. Commonly used neural recording devices can also be integrated with our array: for example, tetrode bundles or silicon probes could be passed down through holes strategically placed in the array. In the years to come, we anticipate that new technologies, such as bundles of waveguides [20] coupled to miniaturised lasers, and novel surgical technologies such as machines that automatically drill craniotomies, will pave the way towards systematic deployment of such devices at even denser levels throughout distributed neural circuits. Such devices may also serve, in the future, as prototype optical neural control prosthetics, supporting

the development of novel treatment strategies for intractable neurological and psychiatric disorders.

5 Acknowledgments

ESB acknowledges funding by the NIH Director's New Innovator Award (DP2OD002002) as well as NIH grants 1RC1MH088182, 1RC2DE020919, 1R01NS067199 and 1R43NS070453, NSF (0835878 and 0848804), McGovern Institute Neurotechnology Award Program, Department of Defense CDMRP PTSD Program, Human Frontiers Science Program, NARSAD, Alfred P. Sloan Foundation, Jerry and Marge Burnett, SFN Research Award for Innovation in Neuroscience, MIT Media Laboratory, Benesse Foundation and Wallace H. Coulter Foundation, the IET Harvey Prize, NIH 2R44NS070453-03A1. JGB acknowledges the Hugh Hampton Young Fellowship. Thanks to Michael Hemann and Neil Gershenfeld and the Center for Bits and Atoms for use of their respective laboratory facilities.

6 References

[1] Aravanis A.M., Wang L.P., Zhang F., *ET AL.*: 'An optical neural interface: in vivo control of rodent motor cortex with integrated fiberoptic and optogenetic technology', *J. Neural Eng.*, 2007, **4**, (3), pp. S143–S156

[2] Bernstein J.G., Han X., Henninger M.A., *ET AL.*: 'Prosthetic systems for therapeutic optical activation and silencing of genetically-targeted neurons', *Proc. Soc. Photo-Opt. Instrum. Eng.*, 2008, **6854**, p. 68540H

[3] Han X., Qian X., Bernstein J.G., *ET AL.*: 'Millisecond-timescale optical control of neural dynamics in the nonhuman primate brain', *Neuron*, 2009, **62**, (2), pp. 191–198

[4] Adamantidis A.R., Zhang F., Aravanis A.M., Deisseroth K., de Lecea L.: 'Neural substrates of awakening probed with optogenetic control of hypocretin neurons', *Nature*, 2007, **450**, (7168), pp. 420–424

[5] Poher V., Grossman N., Kennedy G.T., *ET AL.*: 'Micro-LED arrays: a tool for two-dimensional neuron stimulation', *J. Phys. D, Appl. Phys.*, 2008, **41**, p. 094014

[6] Xu H., Davitt K.M., Dong W., *ET AL.*: 'Integration of a matrix addressable blue/green LED array with multicore imaging fiber for spatio-temporal excitation in endoscopic biomedical applications', *Phys. Status Solidi c*, 2008, **5**, (6), pp. 2299–2302

[7] Ayling O.G., Harrison T.C., Boyd J.D., Goroshkov A., Murphy T.H.: 'Automated light-based mapping of motor cortex by photoactivation of channelrhodopsin-2 transgenic mice', *Nat. Methods*, 2009, **6**, (3), pp. 219–224

[8] Bernstein J.G., Boyden E.S.: 'Optogenetic tools for analyzing the neural circuits of behavior', *Trends Cogn. Sci.*, 2011, **15**, (12), pp. 592–600

[9] Bernstein J.G., Garrity P.A., Boyden E.S.: 'Optogenetics and thermogenetics: technologies for controlling the activity of targeted cells within intact neural circuits', *Curr. Opin. Neurobiol.*, 2012, **22**, (1), pp. 61–71

[10] Wentz C.T., Bernstein J.G., Monahan P., Guerra A., Rodriguez A., Boyden E.S.: 'A wirelessly powered and controlled device for optical neural control of freely-behaving animals', *J. Neural Eng.*, 2011, **8**, (4), p. 046021

[11] Ayling O.G., Harrison T.C., Boyd J.D., Goroshkov A., Murphy T.H.: 'Automated light-based mapping of motor cortex by photoactivation of channelrhodopsin-2 transgenic mice', *Nat. Methods*, 2009, **6**, (3), pp. 219–224

[12] Boyden E.S., Raymond J.L.: 'Active reversal of motor memories reveals rules governing memory encoding', *Neuron*, 2003, **39**, (6), pp. 1031–1042

[13] Hudson M.C.: 'Calculation of the maximum optical coupling efficiency into multimode optical waveguides', *Appl. Opt.*, 1974, **13**, (5), pp. 1029–1033

[14] Chow B.Y., Han X., Dobry A.S., *ET AL.*: 'High-performance genetically targetable optical neural silencing by light-driven proton pumps', *Nature*, 2010, **463**, (7277), pp. 98–102

[15] Han X., Boyden E.S.: 'Multiple-color optical activation, silencing, and desynchronization of neural activity, with single-spike temporal resolution', *PLoS ONE*, 2007, **2**, (3), p. e299

[16] Wang H., Peca J., Matsuzaki M., *ET AL.*: 'High-speed mapping of synaptic connectivity using photostimulation in channelrhodopsin-2 transgenic mice', *Proc. Natl. Acad. Sci. USA*, 2007, **104**, (19), pp. 8143–8148

[17] Boyden E.S., Zhang F., Bamberg E., Nagel G., Deisseroth K.: 'Millisecond-timescale, genetically targeted optical control of neural activity', *Nat. Neurosci.*, 2005, **8**, (9), pp. 1263–1268

[18] Klapoetke N.C., Murata Y., Kim S.S., *ET AL.*: 'Independent optical excitation of distinct neural populations', *Nat. Methods*, 2014, **11**, (3), pp. 338–346

[19] Chuong A.S., Miri M.L., Busskamp V., *ET AL.*: 'Noninvasive optical inhibition with a red-shifted microbial rhodopsin', *Nat. Neurosci.*, 2014, **17**, (8), pp. 1123–1129

[20] Zorzos A.N., Scholvin J., Boyden E.S., Fonstad C.G.: 'Three-dimensional multiwaveguide probe array for light delivery to distributed brain circuits', *Opt. Lett.*, 2012, **37**, (23), pp. 4841–4843